



Enhancing properties of iron and manganese ores as oxygen carriers for chemical looping processes by dry impregnation



S.K. Haider^a, G. Azimi^b, L. Duan^a, E.J. Anthony^{a,*}, K. Patchigolla^a, J.E. Oakey^a, H. Leion^b, T. Mattisson^c, A. Lyngfelt^c

^a Centre for Combustion, Carbon Capture and Storage, School of Energy, Environment and Agrifood, Cranfield University, Cranfield, Bedfordshire MK43 0AL, UK

^b Department of Environmental Inorganic Chemistry, Chalmers University of Technology, S-412 96 Göteborg, Sweden

^c Department of Energy and Environment, Chalmers University of Technology, S-412 96 Göteborg, Sweden

HIGHLIGHTS

- Oxygen carriers were produced by impregnation of metal ores with iron and manganese oxides.
- The oxygen carriers were examined in a bench scale fluidised-bed reactor for CLOU and gaseous fuel conversion.
- Impregnation of these ores positively influences their mechanical properties.
- Above 850 °C, iron ore based oxygen carriers exhibited full syngas conversion.
- Iron ore impregnated with Mn₂O₃ showed significant CLOU behaviour.

ARTICLE INFO

Article history:

Received 10 May 2015

Received in revised form 20 October 2015

Accepted 22 October 2015

Available online 18 November 2015

Keywords:

CO₂ capture

Chemical looping

Oxygen carriers

Natural ore

Chemical-looping with oxygen uncoupling

ABSTRACT

The use of naturally occurring ores as oxygen carriers in CLC processes is attractive because of their relative abundance and low cost. Unfortunately, they typically exhibit lower reactivity and lack the mechanical robustness required, when compared to synthetically produced carriers. Impregnation is a suitable method for enhancing both the reactivity and durability of natural ores when used as oxygen carriers for CLC systems. This investigation uses impregnation to improve the chemical and mechanical properties of a Brazilian manganese ore and a Canadian iron ore. The manganese ore was impregnated with Fe₂O₃ and the iron ore was impregnated with Mn₂O₃ with the goal of forming a combined Fe/Mn oxygen carrier. The impregnated ore's physical characteristics were assessed by SEM, BET and XRD analysis. Measurements of the attrition resistance and crushing strength were used to investigate the mechanical robustness of the oxygen carriers. The impregnated ore's mechanical and physical properties were clearly enhanced by the impregnation method, with boosts in crushing strength of 11–26% and attrition resistance of 37–31% for the impregnated iron and manganese ores, respectively. Both the unmodified and impregnated ore's reactivity, for the conversion of gaseous fuel (CH₄ and syngas) and gaseous oxygen release (CLOU potential) were investigated using a bench-scale quartz fluidised-bed reactor. The impregnated iron ore exhibited a greater degree of syngas conversion compared to the other samples examined. Iron ore based oxygen carrier's syngas conversion increases with the number of oxidation and reduction cycles performed. The impregnated iron ore exhibited gaseous oxygen release over extended periods in an inert atmosphere and remained at a constant 0.2% O₂ concentration by volume at the end of this inert period. This oxygen release would help ensure the efficient use of solid fuels. The impregnated iron ore's reactivity for CH₄ conversion was similar to the reactivity of its unmodified counterpart. The unmodified manganese ore converted CH₄ to the greatest extent of all the samples tested here, while the impregnated manganese ore exhibited a decrease in reactivity with respect to syngas and CH₄ conversion.

Crown Copyright © 2015 Published by Elsevier Ltd. This is an open access article under the CC BY license (<http://creativecommons.org/licenses/by/4.0/>).

1. Introduction

Chemical looping combustion (CLC) is an emerging technology for high-efficiency fossil fuel conversion with inherent carbon capture. The technology's major advantage centres on its ability to

* Corresponding author at: Combustion and CCS Centre, Cranfield University, Bedford, Bedfordshire MK43 0AL, UK. Tel.: +44 (0) 1234 750111x2823.

E-mail address: b.j.anthony@cranfield.ac.uk (E.J. Anthony).

separate oxygen from air and carry out fuel conversion directly with a hydrocarbon fuel. This avoids post-combustion flue gas treatment and its associated energy penalties [1]. CLC systems are based on already established fluidised-bed technology. While systems have been proposed using fixed and moving bed, and pneumatic transport variants, commonly proposed CLC systems generally comprise two interconnected circulating fluidised-bed reactors. A solid oxygen carrier (typically containing a transition metal oxide) is transferred from one reactor to the other, which provides the oxygen required for combustion. The two fluidised-beds are represented as the air reactor (AR) and fuel reactor (FR). The simplified process is shown in Fig. 1. In the FR, the oxygen carrier (OC) provides oxygen, for combustion of fuel in the absence of air. Following the combustion reaction, the reduced form of oxygen carrier is then transferred to the AR, where it is re-oxidised in air, and the looping process continues [2].

The progress required for industrial applications of CLC centres on the development of suitable oxygen carriers. Research into this field has been prolific, with many possible candidate materials tested [3]. A suitable oxygen carrier material for CLC should be relatively inexpensive, mechanically robust and reactive. The reactivity of oxygen carriers depends on several aspects of the chemistry of materials used, including the reducibility to a lower oxidation state, which facilitates the necessary conversion of fuel to combustion products; and the oxidation potential and behaviour of such materials. Oxygen carriers are required to undergo these reactions continuously over many cycles. It is therefore necessary they possess the required chemistry so that these reactions take place at temperatures appropriate for power generation (800–1100 °C). Research on CLC systems using gaseous fuels has received the bulk of attention so far, but current trends in research are increasingly directed to the use of solid fuels such as coal and biomass. Solid fuel conversion in the CLC process requires the presence of steam and/or CO₂ to gasify the solid fuels and produce the intermediate gaseous products CO and H₂, which can then react directly with the solid oxygen carrier [2]. However, this gasification step is relatively slow, limiting the overall fuel conversion rate [4]. In order to overcome this obstacle, the use of oxygen carrier materials that can decompose at high temperatures and under low oxygen partial pressures thereby releasing gaseous oxygen, can be employed [5]. This CLC process is known as chemical looping with oxygen uncoupling, (CLOU) as it does not depend solely on the in-situ gasification step [6]. Determination of the extent of oxygen release under low oxygen partial pressures is an important test to conduct when screening oxygen carriers for their suitability for the conversion of solid fuels in CLOU processes. Considering these prerequisites for a suitable oxygen carrier, the selection narrows towards a number of key transition metals such as Cu, Ni, Mn, Fe and Co and their corresponding oxide systems. Substantial reviews on these systems as well as naturally occurring materials such as ores and some waste or by-product materials have been investigated, elsewhere for both CLC and CLOU systems [3,7,8].

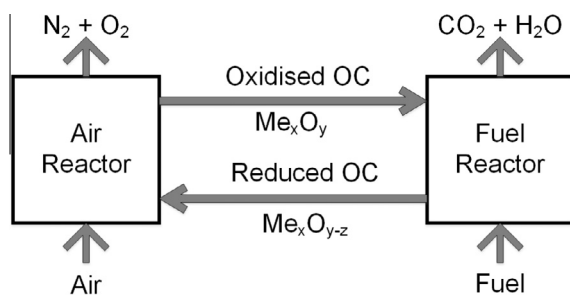


Fig. 1. Simplified schematic of a CLC process.

The earliest example of a CLOU system was the 'Brin process', which was one of the first widely used chemical methods of producing gaseous oxygen. The process utilised the reversible decomposition of barium peroxide to liberate gaseous oxygen and produce barium oxide. It was found that over several cycles the barium oxide systems lost activation, and required catalytic regeneration. The manufacture of gaseous oxygen using this production method ceased in 1906 in favour of the more economically attractive fractionation of liquid air [9]. Though the barium oxide system is not considered today for modern day CLOU processes, due to its toxicity, research continues into prolonging the process life of oxygen carriers. The use of combined materials offers a potential for increasing the process life of oxygen carriers. This is achieved by mixing an active phase material with another or with an inert material as a support. The most well investigated CLOU carrier is currently the Cu/CuO/Cu₂O system due to its favourable reaction kinetics but unfortunately it suffers from agglomeration issues due to the low melting point of Cu (1085 °C), which is close to the practical temperature required for oxygen release [10]. The loss of active oxygen carrier material through processes of attrition, agglomeration and deactivation has also caused research to look towards cheaper materials such as naturally occurring metal ores. Metal ores tend to show inferior chemical reactivity, and their stability and mechanical strength are generally less than synthetically produced ones, although iron ores, comprised mainly of hematite (Fe₂O₃), seem to possess suitable mechanical properties. It has been reported by Mattisson et al. [11] that hematite's methane conversion increases with numbers of oxidation and reduction cycles, though reactivity with methane yields low conversion rates. Nonetheless, the hematite/magnetite (Fe₂O₃/Fe₃O₄) system does not release gaseous oxygen, which is required for rapid and complete solid fuel conversion. Manganese ores have been looked at extensively by Arjmand et al. [12] and they have reported that in general fuel conversion increases with temperatures and that ready liberation of gaseous oxygen at low-oxygen partial pressures is limited to specific manganese ores. Manganese ores are also kinetically hindered during oxidation phases with maximum oxygen partial pressures of 5%. Therefore manganese ores require oxidation to occur at temperatures below 900 °C. Rydén et al. [13] extensively reviewed and investigated the combinations of manganese with other materials, and concluded that manganese in perovskite structures, coupled with calcium-manganates could operate at favourable temperatures and release substantial amounts of gaseous oxygen for CLOU. More notably the combination with iron as another cheap material is evidently interesting for manufacturing low-cost CLOU oxygen carrier. Iron ore's low reactivity and manganese ore's temperature limitations can be improved by combining the metal oxide active phases with other materials. Azimi et al. [14] conducted investigations concerning the Fe–Mn oxide systems looking at the experimental assessment of fuel conversion and oxygen release of varying molar ratios and calcination temperatures of the combined oxide system produced by spray drying. Their study concluded the combined Fe–Mn oxide system is a promising oxide combination, in which the oxidised forms of hematite and bixbyite ((Fe,Mn)₂O₃) can be reduced to magnetite and hausmannite ((Fe,Mn)₃O₄), which yields oxygen release corresponding to 3.3–3.4% change of mass.

Impregnation methods can successfully combine an active phase of a metal oxide onto an inert support material. The technique involves introducing a metal salt solution onto a porous inert support material. The salt solution is first dehydrated to remove the aqueous component and then thermally treated to decompose the salt component, and yield the required loading of active metal oxide. The support material is used to increase the mechanical strength of the oxygen carrier particle, in turn increasing the longevity of carrier particles. Several research groups have used the

impregnation technique in investigations involving the screening of different supports for active phase materials, and their potential as suitable oxygen carriers have been discussed in detail elsewhere [15–17]. Research investigating the use of the impregnation technique to improve the chemical reactivity and mechanical properties of ores, and the general concept of improving ores for oxygen carrier materials has however received limited attention. Gu et al. [18] reports on the use of a 1 kW_{th} interconnected fluidised-bed reactor for solid fuels with a modified iron ore. Dolomite/cement were added to the iron ore by means of mechanical mixing and extrusion. Extruded oxygen carriers once sintered, positively enhanced the iron ores ability to covert coal. Xu et al. [19] has discussed the addition of varying ratios of copper oxide to manganese ore, and found a substantial increase in the conversion of CO even at temperatures as low as 600 °C.

This work reports on an experimental investigation in which transition metal ores of iron and manganese are modified by the impregnation method. Evaluation of these modified ores as low cost oxygen carriers for the CLC process are performed in a lab-scale fluidised-bed reactor. Their reactivity towards gaseous fuels (CH₄ and syngas (CO/H₂ 50%)) and the conversion of these fuels to combustion products is assessed as a function of temperature. In particular, this work seeks to evaluate these oxygen carriers for their CLOU potential for solid fuels by determining the potential gaseous oxygen release in an inert environment to simulate low oxygen partial pressures found in a fuel reactor. Lastly, this study characterises the produced oxygen carriers and their unmodified ore precursors to determine potential improvements in physical and mechanical properties, which could lead to a greater oxygen carrier particle life span and thus evaluate the efficacy of improving ores with the impregnation method.

2. Methods and materials

2.1. Particle preparation

Canadian iron ore supplied by U.S. Steel Canada and Brazilian manganese ore supplied by Mineracao Buritirama, were tested in this work, as a base case and were used as supports to prepare the modified samples. The method of dry-impregnation was selected here, as it allows the active material to be deposited within the pores of the support material. The impregnation was achieved by using two different nitrate salt solutions, to treat the iron and manganese ores. The description of the oxygen carriers tested, and the analysis of the iron and manganese ores, as conducted by ALS Scandinavia AB, is given in Tables 1 and 2 respectively.

The ores were initially heated in a high-temperature furnace at 950 °C for 24 h, to achieve complete oxidation. They were then crushed and sieved to a 125–180 μm size range. The pore volumes were estimated by adding water to a known mass and volume of the ore, to estimate the volume of metal salt solution that could be added. This was estimated to be 29 ml and 39 ml per 100 g of iron and manganese ore respectively. Using this technique, one can avoid over-saturating the ores, which causes non-uniform

Table 1
Oxygen carriers samples.

Designation	Major component	Final impregnated material (%)
Fe100	Canadian iron ore (100%)	N/A
Mn100	Brazilian manganese ore (100%)	N/A
FeMn33	Canadian iron ore (67%)	Mn ₂ O ₃ (33%)
MnFe33	Brazilian manganese ore (67%)	Fe ₂ O ₃ (33%)

Table 2
Composition analyses of ores.

Ore origin	Supplier	Major component	% Total solids (TS)
Canadian iron ore	U.S. Steel Canada	Fe ₂ O ₃	87
		CaO	7
		MgO	2
		MnO	2
		SiO ₂	<1
		K ₂ O	<1
		Al ₂ O ₃	<1
		Na ₂ O	<1
		P ₂ O ₅	<1
		TiO ₂	<1
		Brazilian manganese ore	Mineracao Buritirama
Fe ₂ O ₃	9		
Al ₂ O ₃	7		
SiO ₂	6		
K ₂ O	2		
CaO	<1		
MgO	<1		
Na ₂ O	<1		
P ₂ O ₅	<1		
TiO ₂	<1		

dispersion of the active material loading. For the case of iron ore, an aqueous solution of Mn(NO₃)₂ was prepared by dissolving 78.9 g of Mn(NO₃)₂·4H₂O in 20 ml of deionised water to produce a volume with a concentration of 1.315 g/ml and a corresponding molarity of 5.23 M. A volume of 12 ml of this Mn(NO₃)₂ solution was pipetted onto a 42 g sample of iron ore. The sample was then heated in a furnace at 220 °C for 24 h, to decompose manganese (II) nitrate to manganese dioxide (MnO₂). The sample was then oxidised at 950 °C for 24 h to ensure the production of the fully oxidised state of both the ore support (Fe₂O₃) and impregnated metal oxide (Mn₂O₃) [20]. The process was then repeated twice more until a desired 2:1 M ratio of ore to impregnated metal oxide was achieved. A similar process was used for the preparation of the impregnated manganese ore. 122.1 g of hydrated Iron (III) nitrate (Fe(NO₃)₃·9H₂O) was dissolved in water to make a 136 ml aqueous solution with a corresponding molarity of 3.7 M and 0.8 g/ml concentration. A 13 ml aliquot of the aqueous Iron (III) nitrate (Fe(NO₃)₃) solution was used to impregnate a 34 g sample of the manganese ore support. Following the impregnation step, the sample was placed in a furnace at 250 °C to promote thermal decomposition to Fe₂O₃ [21].

2.2. Experimental setup

Tests were conducted in a bench-scale quartz fluidised-bed reactor, heated by an external vertical furnace as shown in Fig. 2. The reactor length is 820 mm, with a diameter of 22 mm. The reactor has a sintered porous quartz plate, acting as a gas distributor located 370 mm from the base. Simulating the different reaction environments of the AR and FR was achieved by subjecting the oxygen carriers to alternating oxidation (5% O₂ by volume) and reduction (CH₄ or CO/H₂ 50%/50% by volume) cycles within the same reactor vessel. N₂ was used as a sweeping gas in between gas phases, and for inert periods to investigate any possible gaseous oxygen release.

Temperature measurements were made above (25 mm) and below (5 mm) the sintered porous plate by K type chromel–alumel thermocouples. The differential pressure was measured above and below the bed by a Honeywell pressure transducer, which has a measurement frequency of 20 Hz. This measurement provided an indication of fluidisation regime, or de-fluidisation. The resultant flue gas was cooled using an electric cooler to achieve by steam

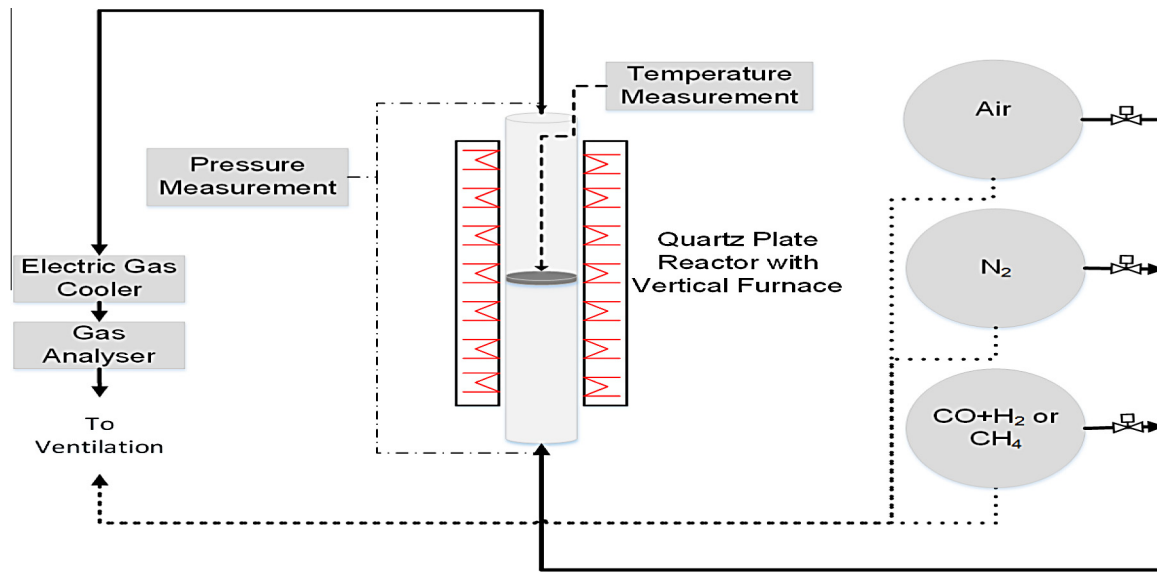


Fig. 2. Overview of laboratory-scale fluidised-bed system.

condensation. The flue gas was then analysed through a Rosemount NGA-2000 gas analyser which measured the volumetric flow-rate and gas concentration on a dry basis. The gas species measured were O_2 , CO , CO_2 and CH_4 .

2.3. Experimental conditions

A sample of oxygen carrier (10 g) was placed on the distributor plate of the quartz reactor. The reactor was then heated up to the first required temperature of 800 °C, at an approximate heating rate of 15 °C/min, whilst in an oxidising atmosphere (5% O_2 in N_2 balance). This 5% O_2 composition was selected to assess the oxygen carrier's ability to oxidise in an oxygen-deficient environment as compared to Air. A 5% oxygen concentration also corresponds to outlet concentrations of an air reactor for a realistic CLC unit [22]. Following the stabilisation of the reactor temperature, the particles were exposed to a N_2 sweeping phase for 60 s, to ensure the oxygen had been fully flushed from the system. The particles were then exposed to the reducing environment for 20 s with methane to assess their fuel conversion ability. Another 60 s period of inert sweeping gas was used to flush any combustible gases, before the oxidising step was repeated. The potential for gaseous oxygen release was assessed, by exposing oxidised oxygen carriers to extended inert periods (360 s) of N_2 gas to promote the release of gaseous oxygen. These reduction/oxidation and extended inert cycles were conducted three times at a given temperature. The temperature was then increased by increments of 50 °C and three reduction/oxidation and inert cycles were conducted at 850, 900, 950 and 1000 °C. The reduction/oxidation cycles were then repeated at temperature increments of 50 °C decreasing from 1000 to 800 °C to determine if the oxygen carrier sample's fuel conversion ability increases with subsequent cycle numbers. Experiments using syngas (CO/H_2 , 50%/50%) followed a similar procedure to that for methane. The oxygen carriers were exposed to a 20 s reduction period with syngas. Due to the high reactivity of the syngas mixture only 1 g of oxygen carrier was used in a bed of 9 g of silica sand. The sand was considered to be an inert bed make-up material and played no role in the reaction chemistry of the oxygen carriers. Table 3 gives data on the alternating gaseous environments, to which the oxygen carriers were subjected. In all environments an aggregative fluidising regime was employed. The flow-rates were selected to correspond approximately to a

Table 3
Experimental gaseous conditions.

Condition	Gas composition (% volume)	Time (s)	Gas flow rate (ml/min)	Temperatures assessed (°C)
Oxidation	O_2/N_2 (5%/95%)	1200	900	800, 850, 900,
Inert	N_2 (100%)	360	600	950, 1000
Reduction	CH_4 (100%)	20	450	
Reduction	CO/H_2 (50%/50%)	20	450	

gas velocity (U) of 5, 8 and 11 times the minimum fluidisation velocity (U_{mf}) for reduction, inert and oxidation steps respectively.

2.4. Oxygen carrier characterisation

The force required to fracture the oxygen carrier particles (crushing strength) was measured using a load cell (Shimpo FGN-5) mounted on a base. Particles of a larger size fraction than those used in the reaction investigation (180–250 μm) were assessed. The particles are placed on the stage, subjected to force until the particles fracture, and the force required to do so is measured. A mean (determined from 30 samples) was used to determine the overall crushing strength. Attrition resistance is measured by the jet cup method as described by [23]. The BET surface area of the oxygen carriers was measured by the nitrogen absorption method in a Micromeritics ASAP 2020 instrument. X-ray diffraction crystallography (XRD) by Siemens D5005 (20–70° θ) and scanning electron microscope (SEM) Philips XL30 with energy-dispersive X-ray (EDX) spectroscopy analysis by Oxford Instruments Swift-ED and analysed by Aztex systems software were utilised to further characterise the physical properties of the particles.

2.5. Data evaluation

Fuel conversion is quantified by the amount of gaseous fuel introduced to the oxygen carrier sample that is converted to carbon-containing combustion products in the outlet stream to provide an indication of the oxygen carrier's reactivity towards the gaseous fuels. The gas conversion γ is calculated using Eqs. (1) and (2) for methane and syngas, respectively, where P_i denotes the partial pressure of the gaseous component. In Eq. (2), the H_2

component of syngas is not taken into account when quantifying gas yield. The conversion of H_2 is assumed to be complete due to the rapid kinetic rate of reaction [24].

$$\gamma_{CH_4} = \frac{P_{CO_2}}{P_{CO_2} + P_{CO} + P_{CH_4}} \quad (1)$$

$$\gamma_{syn} = \frac{P_{CO_2}}{P_{CO_2} + P_{CO}} \quad (2)$$

The degree of oxygen carrier conversion ω_i is defined in Eq. (3), where m_{ox} is the mass of the fully oxidised oxygen carrier material and m_i is the mass of the oxygen carrier at time i .

$$\omega_i = \frac{m_i}{m_{ox}} \quad (3)$$

Mass-based conversion for fuel reduction periods is defined in Eqs. (4) and (5) for methane and syngas, respectively. Oxygen carrier conversion ω_i is calculated as a function of time t_i . m_{ox} is the mass of the fully oxidised sample, n_{out} is the total molar flow of dry gas entering the analyser. M_o is the molar mass of oxygen. p_{tot} is the total partial pressure and $p_{i,out}$ is the partial pressure of component i . It should be noted that the H_2 partial pressure was not specifically measured in the experimental scheme, and instead calculated by assuming equilibrium observing the water gas shift reaction.

$$\omega_i = \omega_{i-1} - \int_{t_{i-1}}^{t_i} \frac{n_{out} M_o}{m_{ox} P_{tot}} (4p_{CO_2,out} + 3p_{CO,out} + 2p_{O_2,out} - p_{H_2,out}) dt \quad (4)$$

$$\omega_i = \omega_{i-1} - \int_{t_{i-1}}^{t_i} \frac{n_{out} M_o}{m_{ox} P_{tot}} (2p_{CO_2,out} + p_{CO,out} + 2p_{O_2,out} - p_{H_2,out}) dt \quad (5)$$

3. Results and discussion

3.1. Particle characterisation

Table 4 shows the values generated by investigations of crushing strength, attrition resistance and surface area. It can be seen that the effect of impregnation of the ores positively influences their physical properties. As crushing strength and attrition resistance are non-standardised tests, the results should be assessed in comparison to other samples in the same experimental series. The results of impregnation of the manganese ores increased the crushing strength by 36% though this substantial increase is not seen in the impregnated iron ore, which demonstrates only a small improvement. However, the increased mechanical strength can be validated by the increase in attrition resistance, where there was a notable decrease in weight percentage loss per hour in the impregnated ores compared to their unmodified precursors. Surface area was measured and seen to increase in the impregnated ores as opposed to their naturally occurring forms.

SEM and EDX analysis was conducted for impregnated FeMn33 and MnFe33 samples and is shown in Figs. 3 and 4. The sample was mounted in an epoxy resin and then cut across the mould to

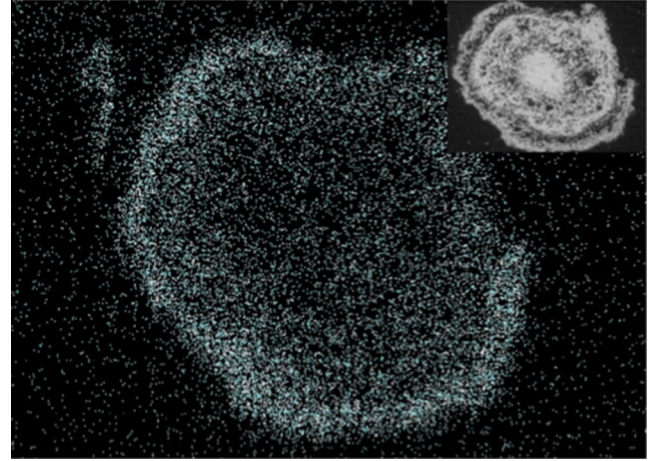


Fig. 3. Mn elemental mapping by EDX of FeMn33 particle.

exhibit a typical particle's cross-sectional area. In Fig. 3 it can be seen that there is significant loading on the outside of the particle. The iron ore had limited porosity compared to the manganese ore. In this instance, the impregnation technique led to a coating on the outside of the iron ore particles, as opposed to penetrating pores. It is considered, that the increased surface area in the impregnated iron ore is largely due to porosity of the impregnated material. It can be seen from Fig. 4 that the MnFe33 particles show a greater degree of uniform dispersion of impregnated iron oxide.

The XRD spectra for the fresh samples of the two impregnated ores are shown in Figs. 5 and 6. The differentiation between peaks corresponding to manganese and iron can be problematic due to their close proximity in periodicity. Furthermore, ores tend to have complex spectra due to the presence of other minerals and various impurities. The major phases are bixbyite (cubic) and hematite (hexagonal-rhombic) in both spectra. In the MnFe33 sample there is evidence of the formation of the non-active phase, Jacobsite, in the cubic arrangement, which is a possible indication of its reduced reactivity.

3.2. Oxygen release

The samples were investigated for fuel conversion and oxygen release by alternating exposure to reduction, inert and oxidation

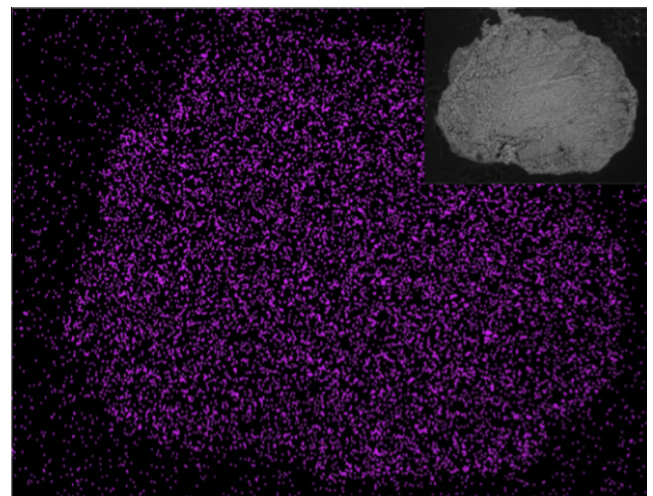


Fig. 4. Fe elemental mapping by EDX of MnFe33 particle.

Table 4
Physical properties of oxygen carriers.

Oxygen carrier	Crushing strength (N)	Attrition rate (wt% loss/h)	BET surface area (m ² /g) (Fresh)
Fe100	1.8	4.3	0.4
FeMn33	1.9	2.7	2.5
Mn100	1.1	4.5	1.8
MnFe33	1.5	3.1	2.4

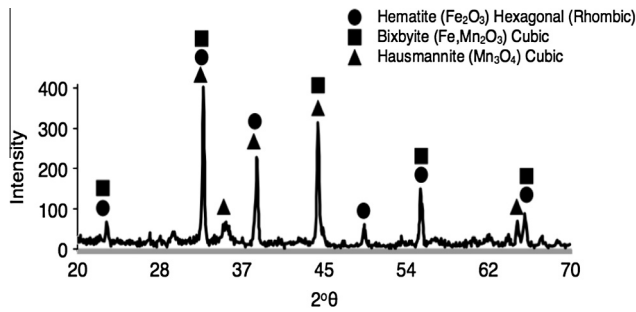


Fig. 5. X-ray diffraction spectra for FeMn33.

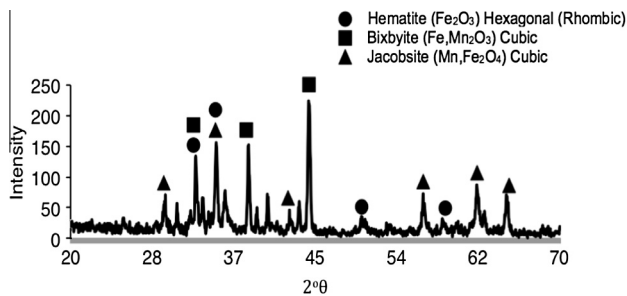


Fig. 6. X-ray diffraction spectra for MnFe33.

gas conditions as described in the experimental procedure. Fig. 7 gives the oxygen concentration as a function of oxygen carrier conversion or reducibility at low-oxygen partial pressure. Conversion yield corresponding to $\omega = 1$ denotes the oxygen carrier is fully oxidised. Extended inert cycles were conducted for a length of 360 s in the presence of N_2 gas as shown in Fig. 8, which shows oxygen concentration or stable oxygen release at low partial pressure as a function of time. As shown in Fig. 7 the samples varied considerably, though it should be noted that the extent to which all samples released oxygen was limited. Fe100 showed a limited but detectable release of gaseous oxygen. The Canadian iron ore has impurities of CaO (8% TS) and MgO (3% TS), calcium has featured as a support in perovskite structured materials, which have been demonstrated to exhibit CLOU behaviour [25]. The content of magnesium oxide in a hematite-based sample has been shown

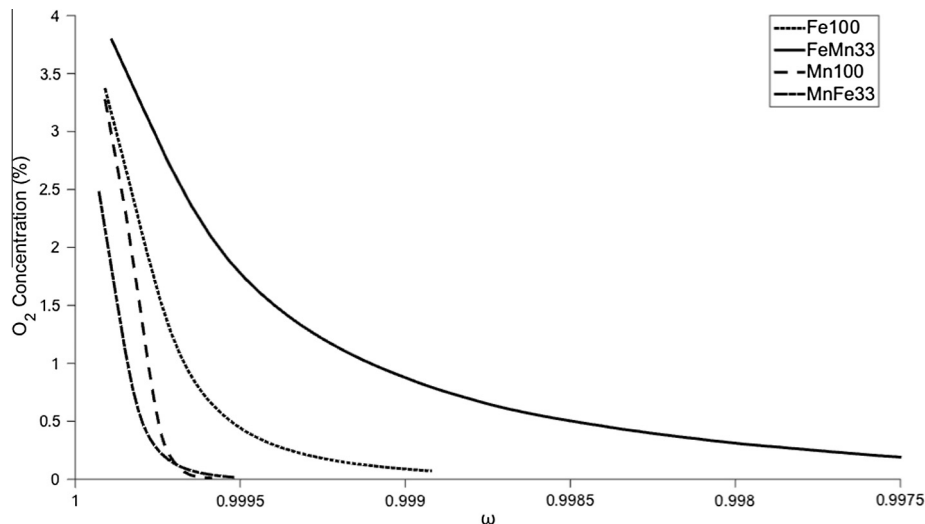


Fig. 7. Oxygen carrier conversion vs. oxygen concentration for inert period at 950 °C.

to increase its oxygen carrying capacity and could contribute to CLOU behaviour [26]. Samples Mn100 and MnFe33 appear to release no gaseous oxygen under inert conditions at 950 °C and MnFe33 with a manganese ore content of 66%, was not expected to release gaseous oxygen, as this is governed by the phase change of bixbyite (Fe,Mn_2O_3) to spinel (Mn,Fe_3O_4). At temperatures above 950 °C, the spinel phase for a manganese content ratio of 66% is stable as per the phase diagram discussed by Azimi et al. [14]. FeMn33 exhibits significant oxygen release compared to the pure iron ore system (Fe100), which is composed of a hematite phase. With a manganese content of 33%, the FeMn33 sample contains both hematite and bixbyite phases. At a temperature of 950 °C, there is a phase boundary with hematite + spinel and hematite + bixbyite phases. The oxygen release exhibited by FeMn33 is consistent, and is attributed to the shift in phase from bixbyite to spinel at this temperature. It has been previously noted [14] that a small increase in temperature will drive the reaction to form the spinel phase and thus release oxygen more readily. FeMn33 releases oxygen for the entire inert period (360 s). This is evident in Fig. 8, and shows the release is consistent at 0.2% by the end of the inert period.

3.3. Syngas conversion

Initial tests investigating the fuel conversion of syngas (CO/H_2 50%/50%) utilised a full bed (10 g) of oxygen carrier. Due to the high reactivity of the syngas fuel with the oxygen carriers investigated, it was difficult to assess the extent of oxygen carrier conversion due to CO being fully converted to CO_2 with a full bed of oxygen carrier. It was, therefore necessary to limit the amount of oxygen carrier to be assessed, by using 1 g of oxygen carrier particles, in a bed of 9 g of silica sand. The gas conversion γ as a function of mass-based oxygen carrier conversion ω is shown in Figs. 9 and 10 at 950 °C and 850 °C, respectively. At 950 °C, FeMn33 marginally outperformed the iron ore system Fe100, though both samples were fully reduced and successfully converted the syngas to combustion products. The manganese-based ores exhibited limited performance in comparison. The pure manganese ore (Mn100) demonstrated a greater extent of syngas conversion than the impregnated ore (MnFe33), which is evident given that Mn100 produced a greater yield in combustion products while the mass based conversion indicate a greater reduction potential than MnFe33. It should be noted, neither sample fully converted the CO to CO_2 , and the extent of conversion was limited to 65% and

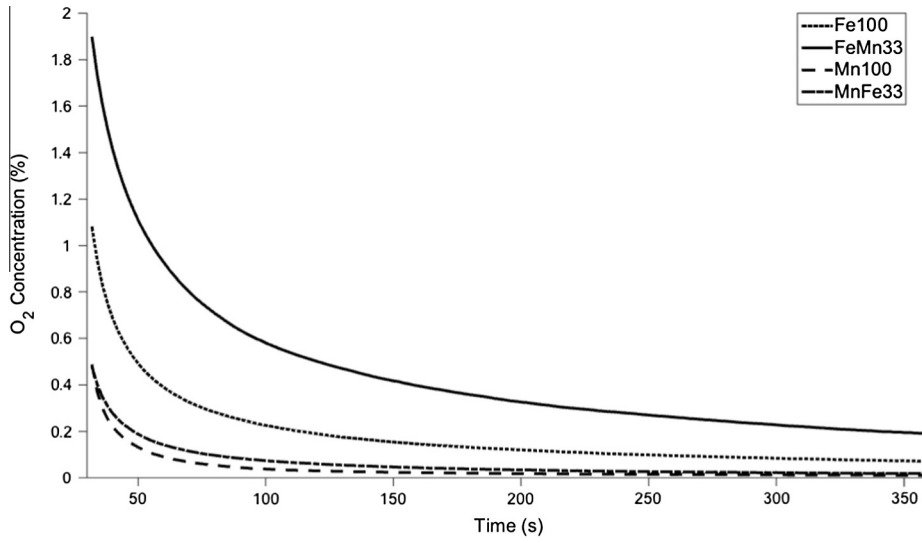


Fig. 8. Oxygen release during inert period (360 s) at 950 °C.

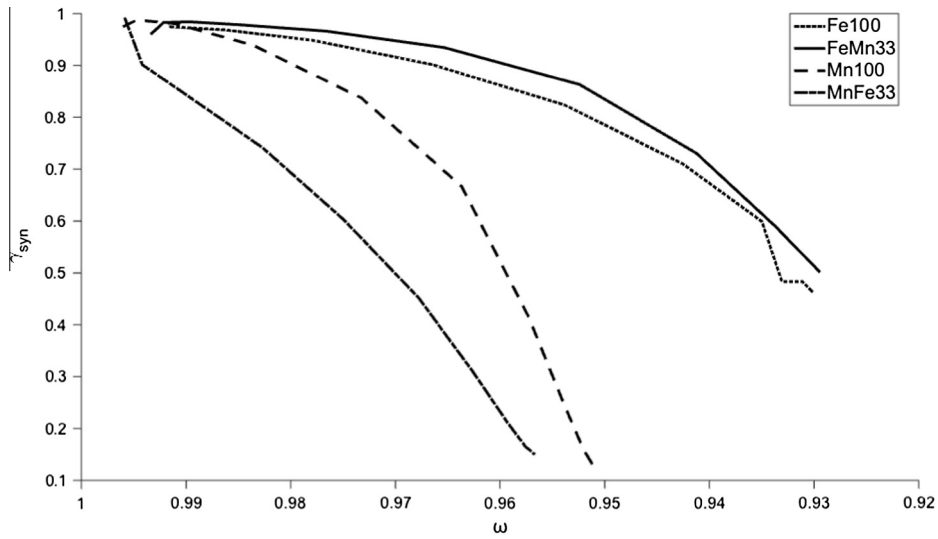


Fig. 9. Oxygen carrier conversion vs. gas yield for reduction with syngas at 950 °C.

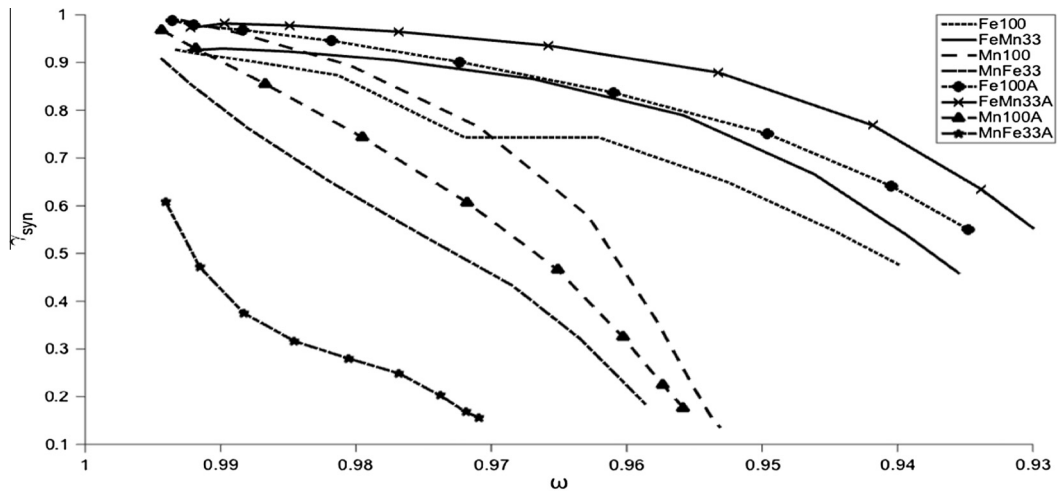


Fig. 10. Oxygen carrier conversion vs. gas yield for reduction with syngas at 850 °C.

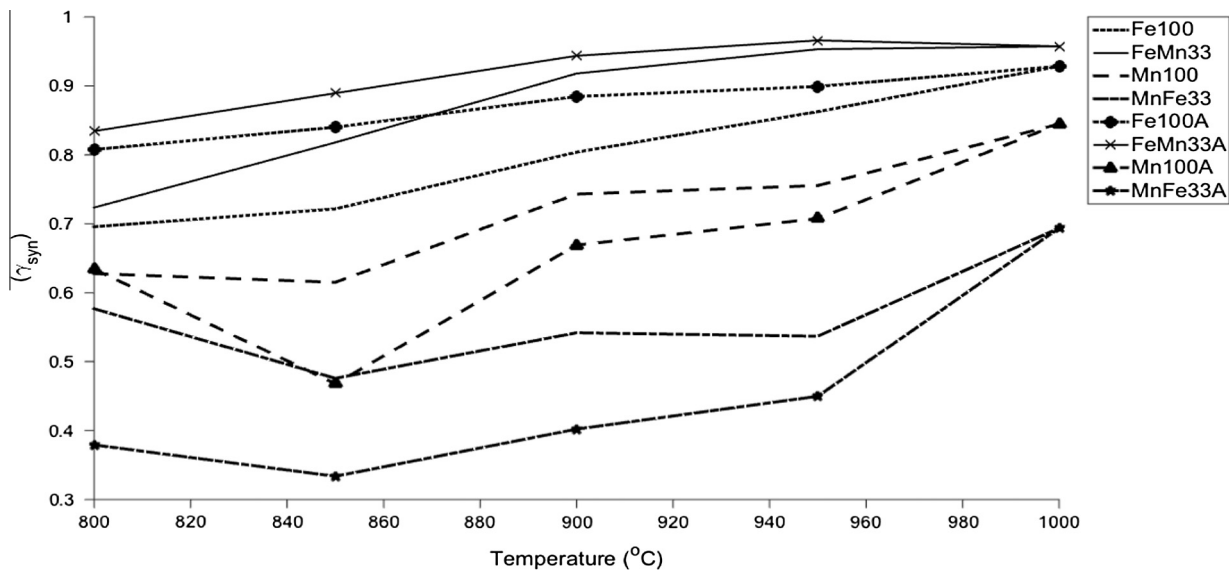


Fig. 11. Average syngas conversion at 800–1000 °C.

45% for Mn100 and MnFe33, respectively, based on outlet concentration (dry basis) measured by the gas analyser.

Syngas conversion at a temperature of 850 °C is shown in Fig. 10. As discussed in the experimental procedure, samples were subjected to fuel cycles from 800–1000–800 °C. In Fig. 10 samples denoting a suffix [A] refer to the gas conversion as a function of mass-based conversion at 850 °C, but with the decreasing temperature step, occurring subsequently to being exposed to the maximum temperature of 1000 °C. The rationale for this procedure was to investigate performance, with increasing cycle numbers. The [A] samples would have been subjected to 19 reduction and oxidation cycles up to this point. The iron-based samples show a clear increase in conversion with cycle numbers, with the impregnated iron ore FeMn33 outperforming its pure ore counterpart. It has been previously discussed [11] that iron-based systems require a number of activation cycles before they achieve stabilised performance. In the iron system, the porous nature of the sample

increases, thus increasing reaction surface area with further oxidation and reduction cycles, although this expansion has limited benefit. Over an increased number of cycles, the micro-pores develop in size and become macro-pores, thus decreasing the surface area and oxygen carrying capacity, and can eventually lead to the oxygen carrier particle disintegrating. Both Mn-based samples exhibit a decline in reactivity and syngas conversion with increased cycle numbers. MnFe33 showed a significant decrease in reactivity, at 850 °C. At this temperature the bixbyite phase formation is prevalent and requires a high rate of reaction to drive the phase change.

The average syngas conversion versus the range of exposure temperatures is shown in Fig. 11. This figure shows that the average syngas conversion of all oxygen carrier samples increases with temperature between 850 and 1000 °C. The samples denoted (A), denoted with corresponding markers, are the values of syngas conversion of the oxygen carrier samples, when decreasing the temperature from 1000 to 800 °C. The iron ore-based oxygen carriers

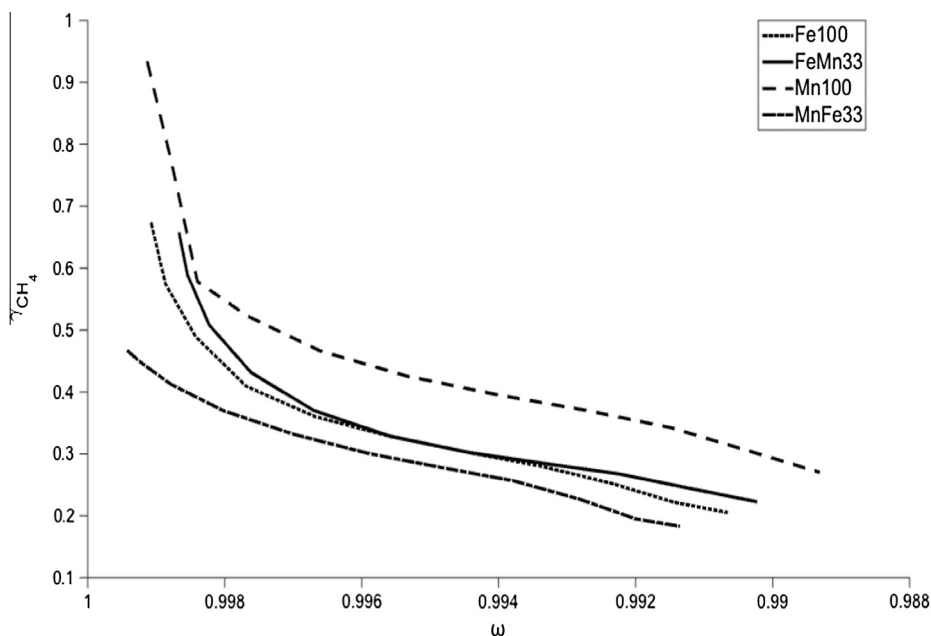


Fig. 12. Oxygen carrier conversion vs. gas yield for reduction with CH₄ at 950 °C.

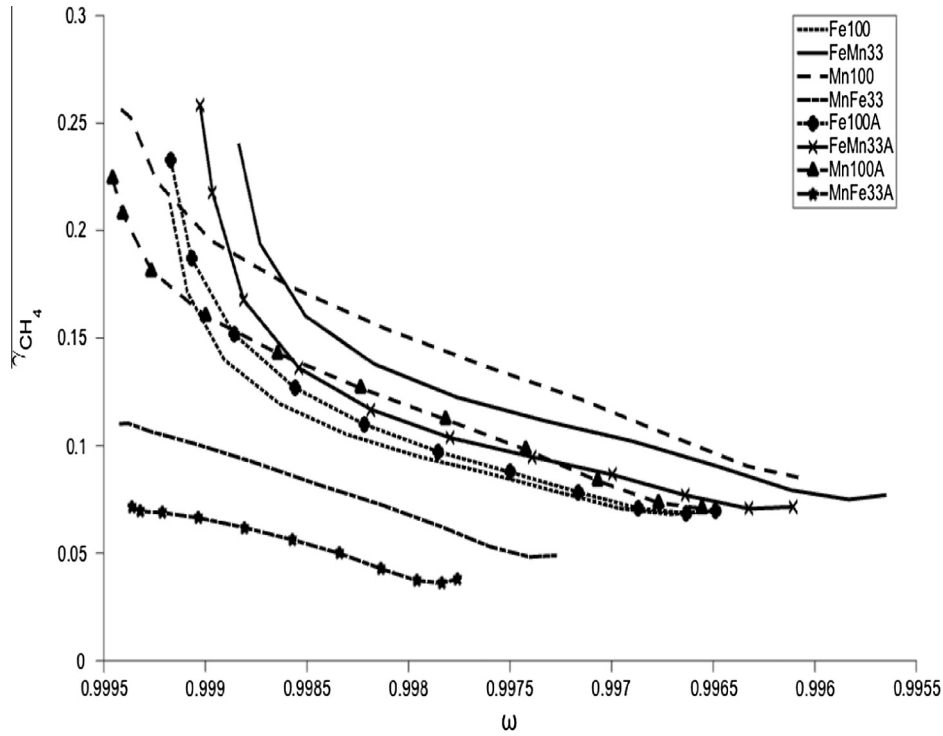


Fig. 13. Oxygen carrier conversion vs. gas yield for reduction with CH_4 at $850\text{ }^\circ\text{C}$.

exhibit enhanced average syngas conversion, due to the preconditioning associated with being exposed to the maximum temperature of $1000\text{ }^\circ\text{C}$ and the effect of further oxidation and reduction cycle numbers. The opposite effect is seen in the manganese ore-based oxygen carriers, where average syngas conversion decreases. In both manganese ore based oxygen carriers, the syngas conversion is higher at $800\text{ }^\circ\text{C}$ than at $850\text{ }^\circ\text{C}$. Given that the oxidation cycles are conducted at the same temperature as reduction with syngas, the enhanced conversion seen at a lower temperature must be due to a greater degree of oxidation occurring at a favourable lower temperature of $800\text{ }^\circ\text{C}$, which facilitates the required phase change of Hausmannite/Spinel to Bixbyite.

3.4. Methane conversion

Figs. 12 and 13 show the gas conversion of methane as a function of mass-based oxygen carrier conversion at $950\text{ }^\circ\text{C}$ and $850\text{ }^\circ\text{C}$, respectively. At $950\text{ }^\circ\text{C}$, the range of samples exhibited comparable conversion and reducibility. However, it should be mentioned that the conversion rates for methane at this temperature were of the order of 30–40%. The manganese ore (Mn100) converted methane to a greater extent than the other samples. Both Fe100 and FeMn33 samples showed very similar extents of conversion. Therefore, it is evident that conversion of methane is not dependent on a gaseous oxygen–methane reaction. At a temperature of $850\text{ }^\circ\text{C}$ methane

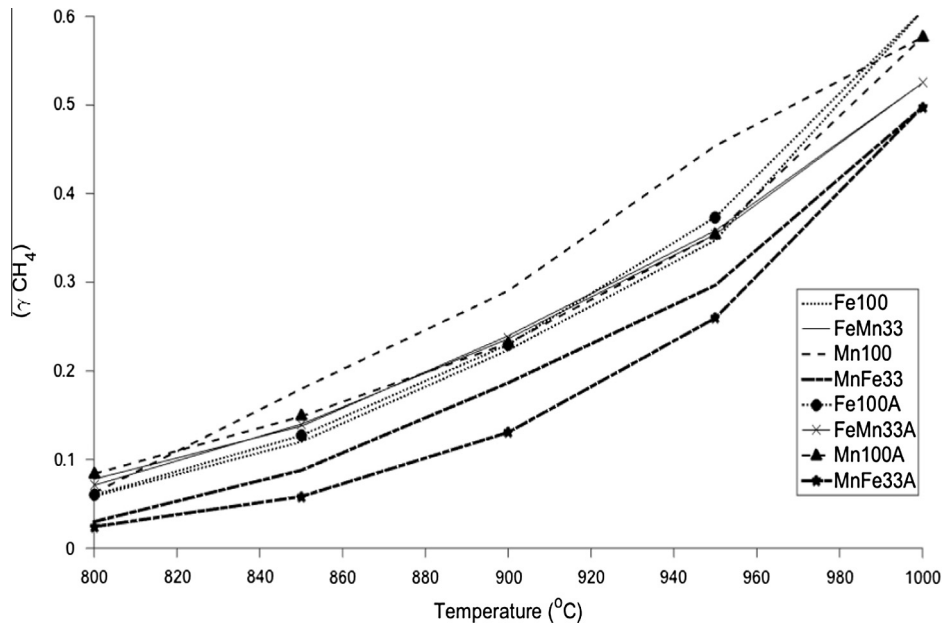


Fig. 14. Average methane conversion at $800\text{--}1000\text{ }^\circ\text{C}$.

conversion becomes progressively limited with conversion rates reduced to below 20%. Here, the increased performance with accumulating cycle numbers was not observed. The increase in micro-pore volume is directly related to the extent of reduction of the oxygen carrier. It is clear that reduction is significantly hindered at this temperature with methane as a reducing gas, and will, therefore, exhibit a lower than expected reactivity.

Average methane conversion against the range of temperatures examined, is shown in Fig. 14. The average conversion of methane increases with temperature; but the effect of increased oxidation and reduction cycles, and exposure to the maximum reaction temperature of 1000 °C does not show the same effect in reactions with CH₄ as it does for syngas. This is most evident in iron ore based carriers, where no significant effect is demonstrated with increasing numbers of reaction cycles. It is also evident that manganese ore based samples exhibit a decrease in methane conversion with increasing cycles number. The unmodified manganese ore still averaged a greater methane conversion compared to the other oxygen carrier samples examined.

4. Conclusions

This study investigates the use of the impregnation method to improve the properties of natural metal ores, in order to produce a suitable oxygen carrier for CLC and CLOU processes. The major findings and conclusions that can be drawn from these investigations are:

The impregnation process positively affected the performance indicators for mechanical strength, with enhancements in attrition resistance and crushing strength. Optical characterisation and surface area by BET N₂ absorption also suggests the porosity of the impregnated material increases.

The manganese-impregnated iron ore, was the only sample to exhibit notable CLOU behaviour with oxygen release of 0.2% at the end of the extended inert cycles. This sample also has the greatest syngas conversion, in comparison to the other samples examined. The effect of increasing cycle number positively influenced the yield of combustion products in iron ore based samples. This behaviour was not observed for the manganese ore based samples, and the effect of increased cycle numbers reduced the ability for gaseous fuel conversion. The conversion of syngas to combustion products by manganese ore based oxygen carriers was not significantly influenced by faster kinetics with higher temperature, as was the case for the conversion of CH₄ with these samples.

Acknowledgements

This work was supported in part by the Engineering and Physical Sciences Research Council (EPSRC grant /K000446/1) through the UK CCS research centre (as part of Phase I project), based on work conducted at Chalmers University of Technology. The work was also financially supported in part by Formas project 2014-1018, and the UKCCSRC under the ECR international travel fund. The iron ore used in this work was supplied by U.S Steel Canada with the help of CanmetEnergy, Natural Resources Canada. Enquiries for access to the data referred to in this article should be directed to researchdata@cranfield.ac.uk.

References

[1] Lyngfelt A, Leckner B, Mattisson T. A fluidized-bed combustion process with inherent CO₂ separation; application of chemical-looping combustion. *Chem Eng Sci* 2001;56:3101–13.

[2] Wang J, Anthony EJ. Clean combustion of solid fuels. *Appl Energy* 2008;85:73–9. <http://dx.doi.org/10.1016/j.apenergy.2007.07.002>.

[3] Adanez J, Abad A, García-Labiano F, Gayán P, de Diego LF. Progress in chemical-looping combustion and reforming technologies. *Prog Energy Combust Sci* 2012;38:215–82. <http://dx.doi.org/10.1016/j.pecs.2011.09.001>.

[4] Saucedo MA, Lim JY, Dennis JS, Scott SA. CO₂-gasification of a lignite coal in the presence of an iron-based oxygen carrier for chemical-looping combustion. *Fuel* 2014;127:186–201. <http://dx.doi.org/10.1016/j.fuel.2013.07.04>.

[5] Imtiaz Q, Broda M, Müller CR. Structure–property relationship of co-precipitated Cu-rich, Al₂O₃- or MgAl₂O₄-stabilized oxygen carriers for chemical looping with oxygen uncoupling (CLOU). *Appl Energy* 2014;119:557–65. <http://dx.doi.org/10.1016/j.apenergy.2014.01.007>.

[6] Mattisson T, Lyngfelt A, Leion H. Chemical-looping with oxygen uncoupling for combustion of solid fuels. *Int J Greenh Gas Control* 2009;3:11–9. <http://dx.doi.org/10.1016/j.ijggc.2008.06.002>.

[7] Lyngfelt A. Oxygen carriers for chemical looping combustion – 4000 h of operational experience. *Oil Gas Sci Technol – Rev d'IFP Energies Nouv* 2011;66:161–72. <http://dx.doi.org/10.2516/ogst/201003>.

[8] Imtiaz Q, Hosseini D, Müller C. Review of oxygen carriers for chemical looping with oxygen uncoupling (CLOU): thermodynamics, material development, and synthesis. *Energy Technol* 2013;1:633–47. <http://dx.doi.org/10.1002/ente.201300099>.

[9] Jensen WB. The origin of the Brin process for the manufacture of oxygen. *J Chem Educ* 2009. <http://dx.doi.org/10.1021/ed086p1266>.

[10] Gayán P, Adanez-Rubio I, Abad A, De Diego LF, García-Labiano F, Adanez J. Development of Cu-based oxygen carriers for chemical-looping with oxygen uncoupling (CLOU) process. *Fuel* 2012;96:226–38. <http://dx.doi.org/10.1016/j.fuel.2012.01.021>.

[11] Leion H, Mattisson T, Lyngfelt A. Use of ores and industrial products as oxygen carriers in chemical-looping combustion use of ores and industrial products As oxygen carriers in chemical-looping combustion. *Energy Fuels* 2009;23:2307–15. <http://dx.doi.org/10.1021/ef8008629>.

[12] Arjmand M, Leion H, Mattisson T, Lyngfelt A. Investigation of different manganese ores as oxygen carriers in chemical-looping combustion (CLC) for solid fuels. *Appl Energy* 2014;113:1883–94. <http://dx.doi.org/10.1016/j.apenergy.2013.06.015>.

[13] Rydén M, Leion H, Mattisson T, Lyngfelt A. Combined oxides as oxygen-carrier material for chemical-looping with oxygen uncoupling. *Appl Energy* 2014;113:1924–32. <http://dx.doi.org/10.1016/j.apenergy.2013.06.016>.

[14] Azimi G, Leion H, Rydén M, Mattisson T, Lyngfelt A. Investigation of different Mn–Fe oxides as oxygen carrier for chemical-looping with oxygen uncoupling (CLOU). *Energy Fuels* 2013;27:367–77. <http://dx.doi.org/10.1021/ef301120r>.

[15] Abad A, Adanez J, García-Labiano F, de Diego LF, Gayán P, Celaya J. Mapping of the range of operational conditions for Cu-, Fe-, and Ni-based oxygen carriers in chemical-looping combustion. *Chem Eng Sci* 2007;62:533–49. <http://dx.doi.org/10.1016/j.ces.2006.09.019>.

[16] Mattisson T, García-Labiano F, Kronberger B, Lyngfelt A, Adanez J, Hofbauer H. Chemical-looping combustion using syngas as fuel. *Int J Greenh Gas Control* 2007;1:158–69. [http://dx.doi.org/10.1016/S1750-5836\(07\)00023-0](http://dx.doi.org/10.1016/S1750-5836(07)00023-0).

[17] Sedor KE, Hossain MM, de Lasa HI. Reactivity and stability of Ni/Al₂O₃ oxygen carrier for chemical-looping combustion (CLC). *Chem Eng Sci* 2008;63:2994–3007.

[18] Gu H, Shen L, Zhong Z, Niu X, Liu W, Ge H, et al. Cement/CaO-modified iron ore as oxygen carrier for chemical looping combustion of coal. *Appl Energy* 2015;157:314–22. <http://dx.doi.org/10.1016/j.apenergy.2015.06.023>.

[19] Xu L, Edland R, Li Z, Leion H, Zhao D, Cai N. Cu-modified manganese ore as an oxygen carrier for chemical looping combustion. *Energy Fuels* 2014;28:7085–92.

[20] Gallagher PK, Schrey F. The thermal decomposition of aqueous manganese (II) nitrate solution. *Thermochim Acta* 1971;2:405–12.

[21] Wiecek-Ciurawa K, Kozak AJ. The thermal decomposition of Fe (NO₃)₃ × 9H₂O. *J Therm Anal Calorim* 1999;58:647–51. <http://dx.doi.org/10.1023/A:1010112814013>.

[22] Arjmand M, Azad A, Leion H, Lyngfelt A, Mattisson T. Prospects of Al₂O₃ and MgAl₂O₄-supported CuO oxygen carriers in chemical-looping combustion (CLC) and chemical-looping with oxygen uncoupling (CLOU). *Energy Fuels* 2011;25:5493–502.

[23] Rydén M, Moldenhauer P, Lindqvist S, Mattisson T, Lyngfelt A. Measuring attrition resistance of oxygen carrier particles for chemical looping combustion with a customized jet cup. *Powder Technol* 2014;256:75–86. <http://dx.doi.org/10.1016/j.powtec.2014.01.085>.

[24] Hallberg P, Jing D, Rydén M, Mattisson T, Lyngfelt A. Chemical looping combustion and chemical looping with oxygen uncoupling experiments in a batch reactor using spray-dried CaMn_{1-x}M_xO_{3-δ} (M = Ti, Fe, Mg) particles as oxygen carriers. *Energy & Fuels* 2013;27:1473–81. <http://dx.doi.org/10.1021/ef3013618>.

[25] De Diego LF, Abad A, Cabello A, Gayán P, García-Labiano F, Adanez J. Reduction and oxidation kinetics of a CaMn_{0.9}Mg_{0.1}O_{3-δ} oxygen carrier for chemical-looping combustion. *Ind Eng Chem Res* 2014;53:87–103. <http://dx.doi.org/10.1016/j.ces.2009.01.059>.

[26] Miller DD, Siriwardane R, Poston J. Fluidized-bed and fixed-bed reactor testing of methane chemical looping combustion with MgO-promoted hematite. *Appl Energy* 2015;146:111–21. <http://dx.doi.org/10.1016/j.apenergy.2015.02.047>.